

A Novel Technique for Link Adaptation Based on Inner Receiver Statistics

Roberto Kagami, Felipe Augusto Pereira de Figueiredo, Victor Hugo Lázaro Lopes and Luciano Leonel Mendes

Abstract—The fast-moving evolution of new technologies is driving the future mobile networks to a challenging pursuit for high throughput and reliability. Emerging services will need precise indicators to address contrasting requisites and link adaptation is a cardinal element. The received signal measurements must provide complete information to perform appropriate and timely decisions. Most communication systems employ statistics based on error rates, but it is not sufficient to accomplish all requirements. Additional information is necessary to define the best parametrization for each application. This paper indicates an approach to achieve this goal by monitoring processes directly into the physical layer decoding.

Keywords—Link adaptation, reliability, polar code, SDR, ML, URLLC, ACM, MCS, 5G, BSG, 6G

I. INTRODUCTION

For future mobile networks, the fine-tuning of a large number of parameters will be required for the proper accomplishment of expected use cases. The definition of Physical Layer (PHY) and Medium Access Control (MAC) parameters must be based on new indicators, and not only the Channel Quality Indicator (CQI) provided by the mobile devices. By providing a precise estimation of the channel conditions, the new indicators allow for a better decision regarding which parameters shall be employed in each application scenario.

A major goal in the system parametrization is to define which modulation order and channel coding rate shall be used in a given communication link. Usually, the breaking point Signal-to-Interference-Plus-Noise Ratio (SINR) for each Modulation Coding Scheme (MCS), defined as the SINR that leads to unacceptable error rate, is used as the main data to switch among the available MCS.

Many algorithms use statistics based on errors to establish these breaking points, such as Bit Error Rate (BER) or Block Error Rate (BLER), which is paradoxical when it comes to finding high levels of reliability. The ACK/NACK signals, used in Hybrid Automatic Repeat Request (HARQ) scheme [1], [2], can be used to identify the breaking point SINRs, but this procedure also depends on a high error rate prospect. There are several approaches available in the literature to estimate the SINR using data-aided (DA) classes [3], [4], [5], [6]. The results presented in the literature show that the performance of the SINR estimation improves when previously known transmit data is used in the receiver side.

On the other hand, the main drawback of these approaches is the assumption that the reception processes are near to ideal. Thus, inaccuracies related to channel estimation, for example, are not taken into account. However, these imprecisions can be quite significant, depending on the channel type and mapping

of pilot signals. A more realistic assessment of the system status, with respect to a link condition, can be achieved through the evaluation of events occurring internally in the physical layer. To take the system processing imperfections into account, it is necessary to consider the information available in the reception algorithms used to recover the data.

As long as new services arise from the predicted mobile networks scenarios, as the Ultra Reliable and Low Latency Communications (URLLC), innovative systems and algorithms are demanded to meet all requirements. Challenging issues are raised with this type of service, including redundancy, error rate analysis and link adaptation [7], [8], [9]. The lack of more complete and supportive information about link and system conditions in this scenario is the motivation of this work.

The subject of this work is the improvement of link status analysis, creating an indicator to select the most efficient MCS index option, considering higher levels of reliability when internal processing inaccuracies are present. The expected indicator has to estimate the real error tendency of a link according to the chosen coding and modulation scheme. It must indicate a faster and more precise representative sample of a low error rate. It must infer an error possibility before its occurrence. Based on these fundamentals, the proposed indicator is implemented using an Orthogonal Frequency Division Multiplexing (OFDM) system environment, but it can also be employed in Single Carrier (SC) schemes. Other link adaptation controls were applied for analysis and comparison with respect to throughput and reliability.

To achieve the described objectives, the remaining of this paper is organized as follows: Section II describes related works, summarizing the advantages and disadvantages of the analyzed schemes. Section III presents the approach to define the indicator introduced in this work, while Section IV depicts the system model and performance evaluation. Section V presents the results and Section VI concludes this paper.

II. RELATED WORKS

Since the advent of 5G networks, with the introduction of network slicing and multiple scenarios, researchers are contributing with new methods to improve the CQI estimation. Apart from the SINR evaluation and CQI definition, that take part in the called Inner Loop Link Adaptation (ILLA), the link adaptation control can consider an Outer Loop Link Adaptation (OLLA) mechanism to compensate measurements and processing inaccuracies [10], [11]. A final definition criteria depends on BLER target and throughput maximization.

The conventional OLLA evaluation establishes margins which are conditioned by statistics. If the discrepancy between

the estimation and target is high, the process can introduce a slow convergence. It can face an even worse scenario depending on the channel variability [12]. The offset margins introduced by OLLA to compensate ILLA inaccuracies can establish considerable variations (from 10% to 30%) [13].

Other algorithms available in the literature can achieve a better performance by using the statistics of the received data. One example is the algorithm based on Bayesian learning proposed in [14]. However, in this case, the simulated target BLER values (0.1 to 0.3) are not considered as a high reliability service category. The OLLA convergence speed can also be accelerated by adjusting the initial offset parameter, as described in [15]. This approach indicates how important is a precise and successful initial CQI estimation in the ILLA.

Proposed methods applying Machine Learning (ML) have emerged to improve link adaptation efficiency, achieving successful results [16]. In [17], Reinforcement Learning (RL) techniques are applied. Many other machine learning procedures are used to optimize the OLLA convergence and performance [18], [19], [20]. However, better results could be achieved using more robust inner information.

III. ERROR CORRECTION AMPLITUDE INDICATOR

The traditional ILLA feedback is based on a lookup table where an SINR determines a CQI index. Empirically, the breaking point SINR for each MCS can be found by varying the SINR while computing the average error rate, as can be seen in Figure 1. When the SINR approaches its breaking point, the error probability increases, indicating a decrement in the Quality of Service (QoS).

After mapping these values, safety margins and hysteresis can be applied according to the degree of reliability, required data rate and QoS factors that manage the current service. As can be seen, the lack of information about what is happening immediately before the occurrence of errors creates a blind region to estimate the error probability and the reliability degree. In this paper, we propose to use the statistical information available on the receiver side to create a better mapping of the quality of the link over the SINR, as depicted in Figure 2.

In the bit detection processing, the involved operations carried out by the PHY decoder are capable of generating information about corrected errors. When a Forward Error Correction (FEC) scheme indicates the number of bits successfully corrected, this data is directly provided. Some Reed-Solomon encoding implementations, e.g., and Intellectual Property (IP) blocks provide this information.

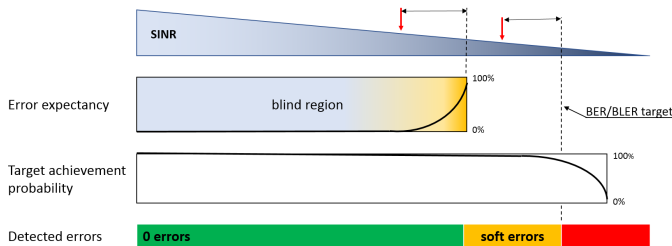


Fig. 1: Breaking point estimation based only in the SINR.

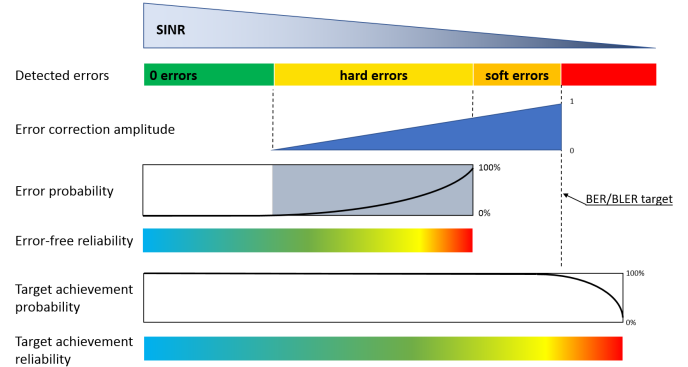


Fig. 2: Breaking point estimation based on the inner receiver statistics.

Otherwise, in schemes like Low Density Check Parity Code (LDPC) and Polar Code, a data preprocessing is necessary to calculate this value. In these cases, considering hard decoding as a detection processing without correction algorithms, a signal can be created comparing this detection with the complete algorithm detection to estimate a reliability level.

According to this approach, an indicator named Error Correction Amplitude (ECA) is introduced. As a definition, it can be stated as:

ECA is the intervention degree applied by the decoding system compared to the detection without correction algorithms or probabilistic analysis techniques.

In practical terms, this indicator can be used to measure the proximity that the decoding system is from an error occurrence or from an expected error rate value.

IV. SYSTEM MODEL AND PERFORMANCE EVALUATION

Actually, polar encoding is used in Fifth Generation of Mobile Networks (5G) channel control messages. However, it is a promising technique to be employed in data channels for future mobile networks. Hence, a model to generate the *ECA* index is proposed based on this technique, using the block diagram shown in Figure 3.

After the channel estimation and the equalization process, the demapper retrieves the data for the Logarithmic Likelihood Ratio (LLR) evaluation, which will be used by the Polar decoder to recover the transmitted bit-stream. In parallel, the hard decoder provides non-corrected data. It is a simple task, demanding very low processing resources. Lookup tables can be used, for instance. The *ECA* processing block compares the sequences obtained in each chain and evaluates the Hadamard distance between them.

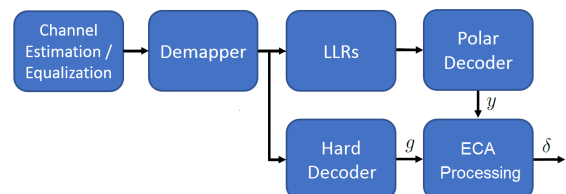


Fig. 3: Block diagram for generating the *ECA* index.

The Polar Coding systems were implemented using the AFF3CT library [21]. It is open-source software coded in C++, licensed by Massachusetts Institute of Technology (MIT), which supports a wide variety of FEC algorithms. Four modulation orders, varying from Quadrature Phase-Shift Keying (QPSK) up to 256-Quadrature Amplitude Modulation (QAM), are combined with 9 different codes rates to generate 22 MCSs. This distribution scheme was elaborated only for validation and proof of concept purposes. Table I presents all MCSs considered in this paper.

TABLE I: MCS definition and breaking point SINR, assuming a codeword length of $N = 2048$ bits.

MCS	Modulation	K	Spectral Effic. (bits/s/Hz)	SINR (10^{-6})
1	QPSK	1024	1.0000000	3.8 dB
2	QPSK	1192	1.1640625	4.6 dB
3	QPSK	1368	1.3359375	5.5 dB
4	QPSK	1536	1.5000000	6.2 dB
5	QPSK	1704	1.6640625	7.3 dB
6	QPSK	1792	1.7500000	7.8 dB
7	16-QAM	1024	2.0000000	10.3 dB
8	16-QAM	1192	2.3281250	11.3 dB
9	16-QAM	1368	2.6718750	12.2 dB
10	16-QAM	1536	3.0000000	13.2 dB
11	16-QAM	1704	3.3281250	14.3 dB
12	16-QAM	1792	3.5000000	14.9 dB
13	64-QAM	1280	3.7500000	16.1 dB
14	64-QAM	1368	4.0078125	16.8 dB
15	64-QAM	1480	4.3359375	17.9 dB
16	64-QAM	1600	4.6875000	18.9 dB
17	64-QAM	1704	4.9921875	19.7 dB
18	64-QAM	1792	5.2500000	20.4 dB
19	256-QAM	1368	5.3437500	24.4 dB
20	256-QAM	1536	6.0000000	25.3 dB
21	256-QAM	1704	6.6562500	26.4 dB
22	256-QAM	1792	7.0000000	27.1 dB

A transceiver, implemented using Software-Defined Radio (SDR) and GNU Radio [22], has been used to evaluate the performance of the proposed indicator under real operating conditions. Figure 4 depicts the block diagram of the test setup.

For each fixed MCS index, the SINR control block automatically sets the Additive White Gaussian Noise (AWGN) power level by sweeping the α parameter and sends the real SINR value to the data acquisition block. The reception block processes the ECA and the average BER, delivering the results synchronously to the data acquisition block. The reception block also configures its current MCS index via the control channel and the payload data is used to calculate the BER statistics. This collected data is shown in Figure 5.

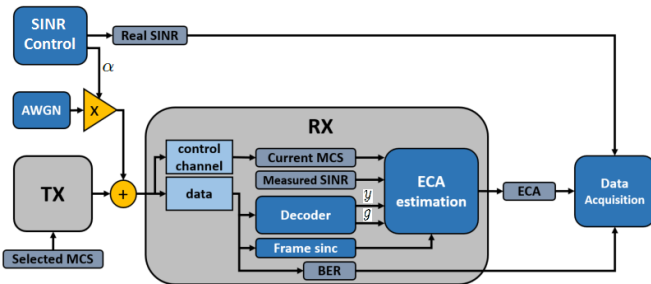


Fig. 4: Data collection diagram.

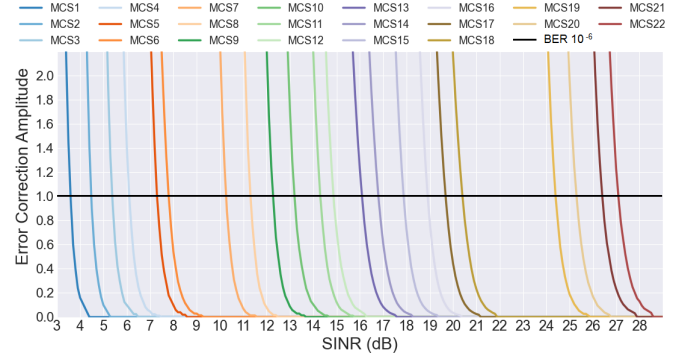


Fig. 5: ECA vs SINR.

The ECA (δ) calculation is executed for each frame and can be determined using (1).

$$\delta = \frac{\sum_{i=1}^m |y_i - g_i|}{\Lambda}, \quad (1)$$

where g_i is the i -th bit produced by the hard decoding, y_i is the i -th bit produced by the soft decoding and m is the number of payload bits in the frame. The Λ parameter is the maximum number of hard bit errors allowed in the frame to achieve the soft BER target. This parameter is determined applying a fixed SINR (Table I) for each MCS index, obtained via simulations. Considering the lower spectral efficiency, $\approx 10^9$ bits were computed to establish a reasonable average value of Λ . With this procedure, the ECA index is linked to a target BER of 10^{-6} . Lower target BER can be used.

In order to evaluate the performance of the proposed SINR approach, errors were introduced in the SINR measurements. The simulations do not include interference. To provide a controlled environment, only white gaussian noise is added. Two measurement inaccuracies were inserted: a nonlinear distortion and an overestimation.

When SINR measurement is obtained using pilots, preambles or cyclic prefixes, the imprecision of channel estimation and interpolation processes are not taken into account. In this case, the overestimated SINR option simulates a situation where the SINR value, measured by the reception block, is 0.5 dB better than the real one provided by the control block.

The nonlinear distortion comes from the average ratio of the symbol power to the error power. The error is the difference between the received data symbols and the decided symbols from the constellation grid. Using (2), the SNR value of a k th received symbol is based on the squared error, given by [23]:

$$\|e_k\|^2 = a_k + b_k, \quad (2)$$

where

$$a_k = \begin{cases} (|\Re(x_k)| - |\Re(\hat{x}_k)|)^2, & \text{if } |\Re(x_k)| \leq d_{\max} \\ (|\Re(x_k)| - d_{\max})^2, & \text{otherwise,} \end{cases} \quad (3)$$

$$b_k = \begin{cases} (|\Im(x_k)| - |\Im(\hat{x}_k)|)^2, & \text{if } |\Im(x_k)| \leq d_{\max} \\ (|\Im(x_k)| - d_{\max})^2, & \text{otherwise,} \end{cases} \quad (4)$$

with x_k is the k th received symbol, \hat{x}_k is the closest symbol in the M -QAM constellation and d_{\max} is the maximum absolute value of the current constellation coordinate. The average SINR per frame is defined as

$$\gamma_{dB} = 10 \log \left(\frac{\sum_{k=1}^n \|e_k\|^2}{n} \right), \quad (5)$$

where n is the number of received symbols in the frame. When a received symbol crosses the constellation grid, an incorrect error value is generated. The difference between the real SINR, provided by the SINR control block, and the measured SINR with imperfections, provided by the reception block, is shown in Figure 6. For comparison purposes, three different modes were implemented to control the link adaptation. The system diagram is shown in Figure 7. To evaluate only the results provided by the ILLA, there is no OLLA scheme. Based on SINR and ECA, a plain operation is adopted, where the MCS index can remain unchanged or it can be increased or decreased by one unit, depending on the target achievement. To reduce the control complexity, high mobility characteristics were not considered. The decision is processed at the end of each frame.

To proceed with the link adaptation control, the estimated MCS index is sent via the loop back to the transmission block. The MCS index configuration is synchronously applied during one entire frame length.

The direct control mode chooses the MCS index based on the breaking point SINR according to the lookup table (column 5 in Table I). The hysteresis control mode also employs the same lookup table. However, an offset (+1dB) is added to the breaking point SINR to establish a fall forward action threshold. An offset (+0.5dB) is also added to the breaking point SINR to establish a fallback action threshold. It creates a safety margin and lower variance.

The ECA control mode defines an immediate fallback action if its value is greater than 1.0. The fall forward action, on the other hand, depends on the lookup table based on data shown in Figure 5. The ECA value is estimated addressing this lookup table with the current MCS index increased by one unit. The fall forward is executed whenever this estimated ECA value is smaller than 1.0.

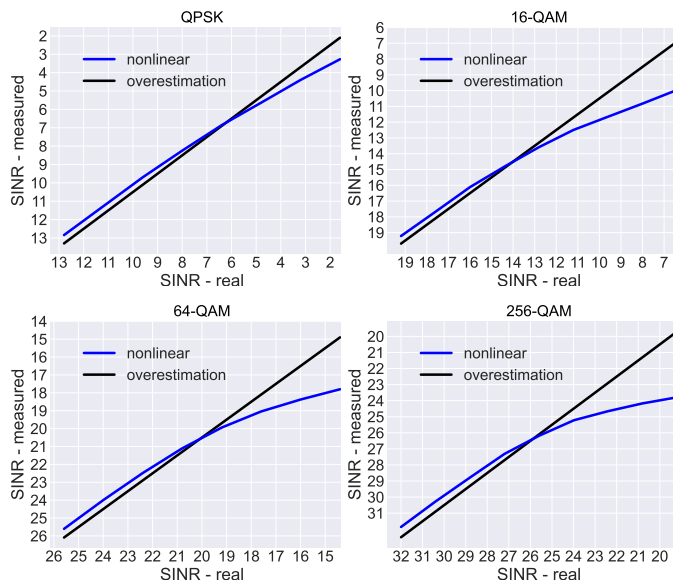


Fig. 6: Measured SINR with imperfections.

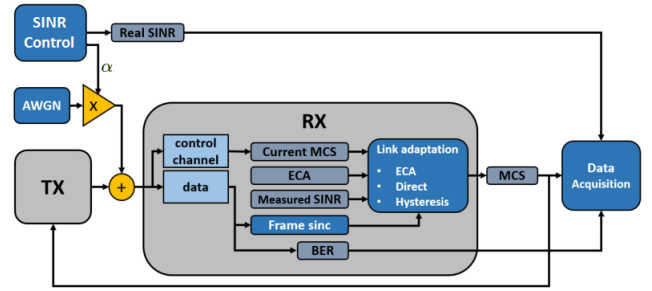


Fig. 7: System diagram.

V. RESULTS

The SINR control block automatically provides the α and real SINR values, as can be seen in Figure 7. The setup range is from 4.2dB to 27.5dB with steps of 0.1dB. A payload data comprises 21670 symbols per frame. The number of elements used to establish average values is 600 frames per SINR step. The achievement index is the average ratio of successful target achievement occurrence ($BER < 10^{-6}$) to the total events. One evaluation is executed per SINR step. As the channel is AWGN, parameters like the number of pilots, Cyclic Prefix (CP) and subcarrier frequency spacing do not affect the results.

Figure 8 shows the results for the three control modes using SINR values with overestimation. Figure 9 exhibits the obtained results for the three modes using SINR values based on grid-based decision method, which generates a nonlinear response. From the simulations in these two scenarios, the total transmitted bits for each type of MCS index control were computed, as well as the BER and respective target achievement index. The tables II and III present these results.

TABLE II: Transmitted bits with overestimated SINR.

Mode	Transmitted bits (Mb)	Achievement %
Direct	11.134	0.43
ECA	10.918	99.57
Hysteresis	10.372	100.00

TABLE III: Transmitted bits with nonlinear measured SINR.

Mode	Transmitted bits (Mb)	Achievement %
Direct	10.982	30.34
ECA	10.826	95.30
Hysteresis	10.172	100.00

As can be seen in Figures 8 and 9, most of the time the direct control mode exceeds the target limit. Collecting the number of transmitted bits, for the case of SINR measurement with overestimation error, the ECA control mode provided a 5.26% gain compared to the hysteresis control mode.

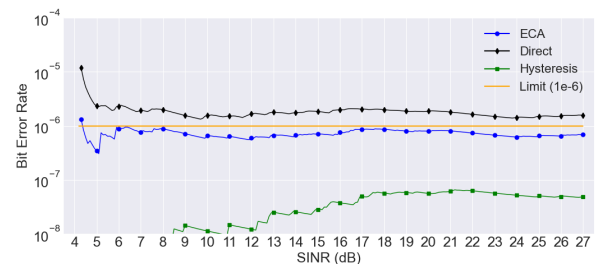


Fig. 8: BER using the overestimated SINR (0.5 dB).

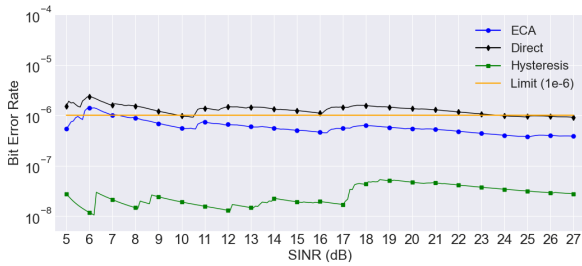


Fig. 9: BER using SINR with nonlinear response.

Similarly, when nonlinear error is applied, a 6.43% gain is verified. The direct and hysteresis control mode could be tuned to equalize the gains. However, this procedure would only fit these particular situations. Using the ECA, the target is achieved automatically for different scenarios.

As can be seen in Figure 6, the estimation error is significant in regions after fallback limits. A fast-changing link condition and delayed fallbacks can establish even greater gains.

Scrutinizing the data close to the BER target limit, it is evinced that the number of hard bit errors is hundreds of times greater than the number of soft bit errors. As a result, this attribute provides faster statistics about low error rates.

Figure 10 shows some examples of BER information obtained via the ECA indicator. It is a robust information, considering the amount of received bits.

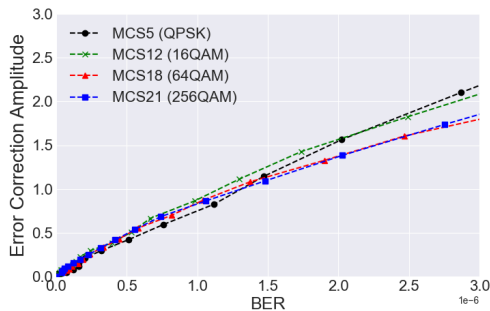


Fig. 10: Measured ECA vs soft BER.

VI. CONCLUSION

The simulations show that the MCS control, using the ECA indicator for the link adaptation, improves the throughput by keeping the demanded reliability strictly. The proposed indicator is consistent with expected attributes. It estimates the real error tendency and indicates a faster and more precise sample of low error rates. It can infer error possibilities before the occurrence, extracting BER statistics with low processing and without payload consumption. For future work, other coding techniques, such as LDPC, can use a similar approach. Machine learning techniques can use the proposed indicator as an input element to achieve higher accurate adaptability.

REFERENCES

[1] T. Ohseki and Y. Suegara, “Fast outer-loop link adaptation scheme realizing low-latency transmission in LTE-Advanced and future wireless networks,” in *2016 IEEE Radio and Wireless Symposium (RWS)*, 2016, pp. 1–3.

[2] M. Deghel, S. E. Elayoubi, A. Galindo-Serrano, and R. Visoz, “Joint Optimization of Link Adaptation and HARQ Retransmissions for URLLC Services,” in *2018 25th International Conference on Telecommunications (ICT)*, 2018, pp. 21–26.

[3] A. M. Khan, V. Jeoti, M. Z. U. Rehman, M. T. Jilani, O. Chughtai, and M. H. Rehmani, “Pilot-Based Time Domain SNR Estimation for Broadcasting OFDM Systems,” *Journal of Computer Networks and Communications*, vol. 2018, p. 9319204, May 2018. [Online]. Available: <https://doi.org/10.1155/2018/9319204>

[4] A. Aloui, O. B. Rhouma, and C. Rebai, “Preamble based SNR estimation for IEEE 802.15.4g MR-OFDM,” in *2018 25th IEEE International Conference on Electronics, Circuits and Systems (ICECS)*, 2018, pp. 325–328.

[5] S. Malik, S. Portugal, C. Seo, C. Kim, and I. Hwang, “Proposal and performance analysis of a novel preamble-based Signal-to-Noise Ratio (SNR) estimation algorithm,” in *2011 34th International Conference on Telecommunications and Signal Processing*, 2011, pp. 100–103.

[6] S. Baumgartner, G. Hirtz, and A. Baumgartner, “A modified maximum likelihood method for SNR estimation in OFDM based systems,” in *2014 IEEE International Conference on Consumer Electronics (ICCE)*, 2014, pp. 155–158.

[7] J. Khan and L. Jacob, “Link Adaptation for Multi-connectivity Enabled 5G URLLC: Challenges and Solutions,” in *2021 International Conference on Communication Systems Networks*, 2021, pp. 148–152.

[8] S. Nayak and S. Roy, “Novel Markov Chain Based URLLC Link Adaptation Method for 5G Vehicular Networking,” *IEEE Transactions on Vehicular Technology*, vol. 70, no. 12, pp. 12 302–12 311, 2021.

[9] J. Choi, “On Error Rate Analysis for URLLC over Multiple Fading Channels,” in *2020 IEEE Wireless Communications and Networking Conference (WCNC)*, 2020, pp. 1–5.

[10] J. Park and S. Baek, “Two-Stage Thompson Sampling for Outer-Loop Link Adaptation,” *IEEE Wireless Communications Letters*, vol. 10, no. 9, pp. 2004–2008, 2021.

[11] B.-C. et al., “eOLLA: an enhanced Outer Loop Link Adaptation for Cellular Networks,” *EURASIP Journal on Wireless Communications and Networking*, 2016.

[12] M. G. Sarret, D. Catania, F. Frederiksen, A. F. Cattoni, G. Berardinelli, and P. Mogensen, “Dynamic Outer Loop Link Adaptation for the 5G Centimeter-Wave Concept,” in *Proceedings of European Wireless 2015; 21th European Wireless Conference*, 2015, pp. 1–6.

[13] S. Park, R. C. Daniels, and R. W. Heath, “Optimizing the Target Error Rate for Link Adaptation,” in *2015 IEEE Global Communications Conference (GLOBECOM)*, 2015, pp. 1–6.

[14] V. Saxena and J. Jaldén, “Bayesian Link Adaptation under a BLER Target,” in *2020 IEEE 21st International Workshop on Signal Processing Advances in Wireless Communications (SPAWC)*, 2020, pp. 1–5.

[15] A. Durán, M. Toril, F. Ruiz, and A. Mendo, “Self-Optimization Algorithm for Outer Loop Link Adaptation in LTE,” *IEEE Communications Letters*, vol. 19, no. 11, pp. 2005–2008, 2015.

[16] F. J. Martín-Vega, J. C. Ruiz-Sicilia, M. C. Aguayo, and G. Gómez, “Emerging Tools for Link Adaptation on 5G NR and Beyond: Challenges and Opportunities,” *IEEE Access*, vol. 9, pp. 126 976–126 987, 2021.

[17] P. S. J. Khan, and L. Jacob, “Reinforcement Learning Based Link Adaptation in 5G URLLC,” in *2021 8th International Conference on Smart Computing and Communications (ICSCC)*, 2021, pp. 159–163.

[18] M. P. Mota, D. C. Araujo, F. H. Costa Neto, A. L. F. de Almeida, and F. R. Cavalcanti, “Adaptive Modulation and Coding Based on Reinforcement Learning for 5G Networks,” in *2019 IEEE Globecom Workshops (GC Wkshps)*, 2019, pp. 1–6.

[19] P. S. Pati, S. S. Sahoo, D. Krishnaswamy, and R. Datta, “A Novel Machine Learning Approach for Link Adaptation in 5G Wireless Networks,” in *2020 2nd PhD Colloquium on Ethically Driven Innovation and Technology for Society (PhD EDITS)*, 2020, pp. 1–2.

[20] V. Saxena, H. Tullberg, and J. Jaldén, “Reinforcement Learning for Efficient and Tuning-Free Link Adaptation,” *IEEE Transactions on Wireless Communications*, pp. 1–1, 2021.

[21] A. Cassagne, O. Hartmann, M. Leonardon, K. He, C. Leroux, R. Tajan, O. Aumage, D. Barthou, T. Tonnellier, V. Pignoly et al., “AFF3CT: A Fast Forward Error Correction Toolbox!” *SoftwareX*, p. 100345, 2019.

[22] GNU Radio Website, accessed July 2020. [Online]. Available: <http://www.gnuradio.org>

[23] R. Kagami and L. Mendes, “A Low-Complexity Deep Neural Network for Signal-to-Interference-Plus-Noise Ratio Estimation,” in *Anais do I Workshop de Redes 6G*. Porto Alegre, RS, Brasil: SBC, 2021, pp. 1–6. [Online]. Available: <https://sol.sbc.org.br/index.php/w6g/article/view/17227>